Accepted Manuscript

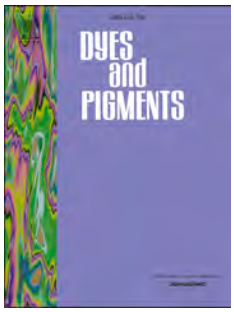

Pyranylidene/thienothiophene-based organic sensitizers for dye-sensitized solar cells

A. Belén Marco, Natalia Martínez de Baroja, José María Andrés-Castán, Santiago Franco, Raquel Andreu, Belén Villacampa, Jesús Orduna, Javier Garín

PII: S0143-7208(18)31630-9

DOI: 10.1016/j.dyepig.2018.09.035

Reference: DYPI 7017

To appear in: *Dyes and Pigments*

Received Date: 25 July 2018

Revised Date: 29 August 2018

Accepted Date: 15 September 2018

Please cite this article as: Marco ABelé, Martínez de Baroja N, Andrés-Castán JoséMarí, Franco S, Andreu R, Villacampa Belé, Orduna Jesú, Garín J, Pyranylidene/thienothiophene-based organic sensitizers for dye-sensitized solar cells, *Dyes and Pigments* (2018), doi: https://doi.org/10.1016/j.dyepig.2018.09.035.

Pyranylidene/thienothiophene-based organic sensitizers for Dye-Sensitized Solar Cells

A. Belén Marco,[a] Natalia Martínez de Baroja,[a] José María Andrés-Castán,[a] Santiago Franco,*[a] Raquel Andreu,*[a] Belén Villacampa,[b] Jesús Orduna,[a] Javier Garín.[a]

[a] Departamento de Química Orgánica, ICMA, Universidad de Zaragoza-CSIC, 50009 Zaragoza, Spain.

[b] Departamento de Física de la Materia Condensada, ICMA, Universidad de Zaragoza-CSIC, 50009 Zaragoza, Spain.

Corresponding author: randreu@unizar.es

Abstract

Novel push-pull systems featuring a 4*H*-pyranylidene donor fragment and thienothiophene as (part of) π-conjugated spacer have been synthesized in order to test their photovoltaic properties. An analogous derivative with two thiophene rings is also included in the study for comparison purposes. The optical and electrochemical properties of the novel D-π-A molecules have been discussed and DSSCs devices based on these dyes have been characterized. The photovoltaic performance is sensitive to the structural modification of the dye: the *tert*-butyl substituents on the pyranylidene moiety and the hexyl chains of the thienothiophene spacer were shown to improve the efficiency. A maximum power conversion efficiency of 6.41% has been achieved.

Keywords:

Dye-sensitized solar cells, push-pull systems, 4*H*-pyranylidene, thienothiophene.

1. Introduction

Solar energy stands out as the most promising renewable source to supplant fossil resources. In this context, organic solar cells (OSCs)[1] and, particularly Dye Sensitized Solar Cells (DSSCs)[2] constitute an interesting alternative due to their high performance and low manufacturing cost.

In DSSCs, the photosensitizing dye is the main component, responsible to determine the light harvesting performance and the final efficiency. Although, at first, ruthenium complexes were widely used as high-efficient sensitizers,[3] and transition metal complexes are still playing a role in DSSC development,[4] over the last decade, metal-free organic dyes have been widely studied and developed as a real alternative. They take advantage of their high molar extinction coefficient, the possibility of tuning their photophysical and electrochemical properties through a suitable molecular design, easy preparation, color, light weight and low-cost production.

The efficiencies of organic dyes have been improving continuously and values up to 14.7 % have already been achieved[5] with collaborative sensitization of a carbazole-derivative dye and a triphenylamine-based one. The development of new organic dyes is still a key to the progress of this field, in order to explore the potentials of new materials as well as to deepen in the relationship between structure and device performance.

Generally, metal-free organic dyes involve an electron donor (D) and an electron acceptor (A) connected by a π-bridge, the so-called D-π-A structure, which promotes an efficient photoinduced intramolecular charge transfer (ICT). It is well known that the structure of the three components of the organic dye has profound repercussions on its performance as sensitizer for DSSCs. A wide number of donors and π-linkers have been exploited, whereas cyanoacrylic acid is often chosen as the electron accepting unit/anchoring moiety, because of

the presence of the electron withdrawing cyano group and its outstanding electron injection properties.[6]

Among electron donors, triphenylamine-based derivatives have been widely used[7] due to their nonplanar structure that prevents the dye aggregation, but other moieties, like dialkylaminophenyl,[8] indoline,[9] carbazole,[10] dithiafulvene[11] or tetrathiafulvalene (TTF)[12] groups have been introduced as efficient donor units.

As concerns the π-bridge, it plays an essential role in tuning the main photochemical properties of the sensitizers,[13] regulating the HOMO-LUMO energy levels and extending the absorption range. Although the thiophene moiety is among the most used conjugated linkers, various heteroaromatic derivatives, such as oligothiophene,[14] thiazol,[15] benzothiadiazole[16] or thienothiophene (TT) have been explored. In particular, thieno[3,2-*b*]thiophene (TT) is an excellent π-spacer[17] that offers fine π-conjugation, low resonance energy per electron and improved thermal stability. In materials chemistry, functionalized TT derivatives have found application, for example, in non-linear optics (NLO),[18] organic light-emitting diodes (OLEDs)[19] or DSSCs,[20] reaching an efficiency value of 9.8 %[20d] for a TT system with a triphenylamine derivative as donor end.

γ-Pyranylidene-containing dyes constitute a class of molecules deeply studied in the field of photonics and organic electronics. Its proaromatic character[21] improves the charge transfer process through the gain in aromaticity. The synthetic versatility provided by the building blocks of this type of compounds allowed the synthesis and characterization of a variety of structures, affording materials with interesting properties, like second-order optical activity[22] or two-photon absorption,[23] and OSCs.[24]

In the last years, the use of this class of derivatives as sensitizer for DSSCs has shown encouraging results, with the 4*H*-pyranylidene moiety acting as donor fragment,[25] as π-spacer[26] or as a core linked to different electron accepting groups in order to tune the

optical absorption of the dyes.[27] Thus, an efficiency of 5.86% has been obtained[25e] for a dye based on a 2,6-diphenyl-4*H*-pyranylidene donor linked to a cyanoacrylic fragment through a thiophene with a trialkylsilylether.

Within this context, having in mind the previously reported work in this field, as well as our experience on the synthesis and characterization of push-pull systems featuring 4*H*-pyranylidene donor fragments with a TT relay for optical applications,[18b-c] we present the synthesis and evaluation of four novel organic dyes (Fig. 1) bearing this proaromatic donor, a TT unit in the π-spacer group and a cyanoacrylic acid as the acceptor/anchoring moiety. To the best of our knowledge, no dyes with a 4*H*-pyranylidene/TT combination in their structure have been studied in relation to their DSSCs activity. An analogous derivative with two thiophene segments connected by an ethylenic unit (-CH=CH-) as the π-linker (compound **4**, Fig. 1) is also included in this study for the sake of comparison. This compound, with an enlarged π-system should lead to a red-shift of dye absorption, together with an adequacy of the HOMO/LUMO ratio of the dye.[20a,28] The hexyl chains attached to the TT spacer (compound **3**) or to thiophene units (compound **4**) may contribute to suppress intermolecular aggregation, increase the solubility of the dyes,[20i,25c] and minimize the charge recombination.[20e-f]

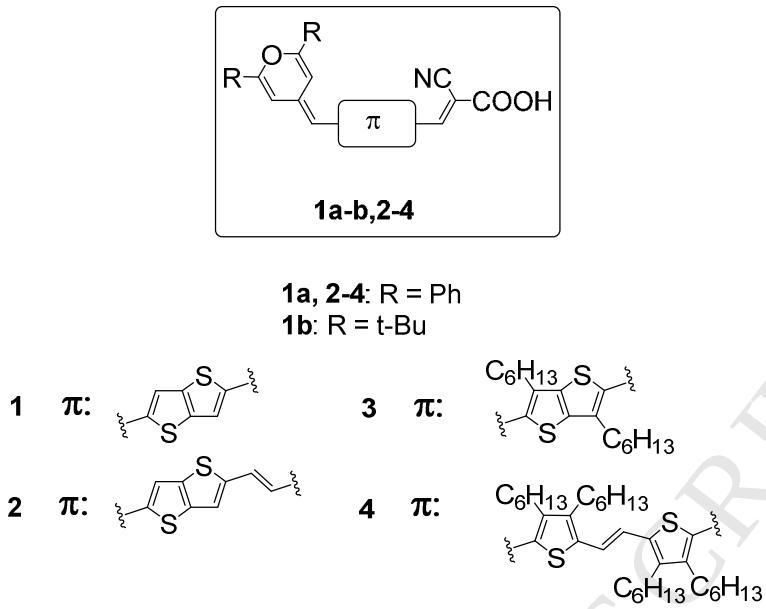

Fig. 1. Molecular structures of the targeted dyes

2. Experimental

2.1. General experimental methods

Infrared measurements were carried out in KBr using a Perkin-Elmer Fourier Transform Infrared 1600 spectrometer. Melting points were obtained on a Gallenkamp apparatus in open capillaries and are uncorrected. ^{1}H-NMR spectra were recorded on a Bruker ARX300, a Bruker AV400, or a Bruker AV500 at 300, 400 or 500 MHz. ^{13}C-NMR spectra were recorded on a Bruker ARX300 or a Bruker AV400 at 75 or 100 MHz respectively; δ values are given in ppm (relative to TMS) and *J* values in Hz. The apparent resonance multiplicity is described as s (singlet), br s (broad singlet), d (doublet), t (triplet), q (quartet) and m (multiplet). ^{1}H-^{1}H COSY experiments were recorded on a Bruker AV400 or a Bruker AV500 at 400 or 500 MHz in order to establish peaks assignment and spatial relationships. MALDI-ToF Mass Spectra were recorded using dithranol as matrix; accurate mass measurements were achieved using PEG as external reference and calibrating with $[PEG+Na]^{+}$. Electrospray mass spectra were recorded on a Bruker Q-ToF spectrometer; accurate mass measurements were achieved using

sodium formate as external reference. UV-Visible spectra were recorded with an UV-Vis UNICAM UV4 spectrophotometer. Fluorescence spectra were obtained in a Perkin Elmer LS50B.

Differential Pulse Voltammetry measurements were performed with a μ-Autolab type III potentiostat using a glassy carbon working electrode, Pt counter electrode, and Ag/AgCl reference electrode. The experiments were carried out under argon in CH_2Cl_2, with Bu_4NPF_6 as supporting electrolyte (0.1 mol L^{-1}). Step potential was 0.01 V and the interval time 0.5 s.

2.2. Device preparation and characterization

See Supporting Information

2.3. Computational details

See Supporting Information

2.4. Starting materials

Compounds **5a**,[18b] **5b**,[18c] **6**,[18b] **9**,[29] **11**[30] and **12**[31] were prepared as previously described.

2.5. Synthesis and characterizations

2.5.1. **3,6-dihexylthieno[3,2-*b*]thiophene-2,5-dicarbaldehyde (10)**

n-BuLi (1.6 M) in hexanes (1.56 mL, 2.5 mmol) was added to a solution of 3,6-dihexylthieno[3,2-*b*]thiophene (**9**) (0.250 g, 0.81 mmol) and previously dried TMEDA (375 μL, 2.49 mmol) in dry hexane (3 mL), at room temperature under argon atmosphere. The mixture was refluxed for 1 h, cooled to room temperature and then to – 40 ºC. Dry THF (4 mL) and dry DMF (205 μL, 2.66 mmol) were added and the mixture was warmed to room temperature for 5 h. 1M HCl (50 mL) was then added and the aqueous phase was extracted with AcOEt (3×50 mL). The organic layer was washed with water (3×50 mL), dried over $MgSO_4$ and evaporated. The crude product was purified by flash column chromatography

(silicagel) with hexane, then hexane/AcOEt (93:7) as the eluent, affording **10** (0.184 g, 0.505 mmol, 62%) as a pale orange powder. Mp 106–108 ºC. IR (KBr) cm^{-1}: 1646 (C=O). ^{1}H-NMR (400 MHz, $CDCl_3$) δ (ppm): 10.16 (s, 2H), 3.11 (t, *J* = 7.5 Hz, 4H), 1.85–1.75 (m, 4H), 1.43–1.27 (m, 12H), 0.88 (t, *J* = 7.5 Hz, 6H). ^{13}C-NMR (100 MHz, $CDCl_3$) δ (ppm): 182.7, 145.1, 144.8, 142.3, 31.4, 29.9, 29.1, 28.1, 22.5, 14.0. HRMS (ESI^+) m/z: found: $[M+H]^+$ 365.1602; molecular formula $C_{20}H_{29}O_2S_2$ requires $[M+H]^+$ 365.1603; found: $[M+Na]^+$ 387.1410; molecular formula $C_{20}H_{28}NaO_2S_2$ requires $[M+Na]^+$ 387.1423.

2.5.2. **5-((2,6-diphenyl-4*H*-pyran-4-ylidene)methyl)-3,6-dihexylthieno[3,2-*b*]thiophene-2-carbaldehyde (7)**

n-BuLi (1.6 M) in hexanes (0.3 mL, 0.45 mmol) was added to a solution of diphenyl(2,6-diphenyl-4*H*-pyran-4-yl) phosphine oxide (**11**) (0.179 g, 0.411 mmol) in dry THF (5 mL) at –30 ºC under argon atmosphere. The solution turned dark green and was stirred at this temperature for 15 min. Then, the solution was slowly added by using a cannula to a solution of dialdehyde **10** (0.150 g, 0.411 mmol) at –30 ºC in dry THF (4 mL), and the mixture was stirred for a further 1 h. A saturated solution of NH_4Cl (50 mL) was then added and the aqueous phase was extracted with AcOEt (3×50 mL). The resulting organic layer was dried over $MgSO_4$ and evaporated. The crude product was purified by flash column chromatography (silicagel) with hexane/AcOEt (95:5) as the eluent, to give **7** (0.107 g, 0.184 mmol, 45%) as a red solid. Mp 152–154 ºC. IR (KBr) cm^{-1}: 1629 (C=O). ^{1}H-NMR (300 MHz, $CDCl_3$) δ (ppm): 10.01 (s, 1H), 7.86–7.81 (m, 2H), 7.80–7.75 (m, 2H), 7.51–7.38 (m, 6H), 7.22 (d, *J* = 1.8 Hz, 1H), 6.51 (d, *J* = 1.8 Hz, 1H), 6.08 (s, 1H), 3.09 (t, *J* = 7.6 Hz, 2H), 1.88–1.78 (m, 2H), 1.73–1.63 (m, 2H), 1.45–1.25 (m, 12H), 0.92–0.82 (m, 6H). ^{13}C-NMR (75 MHz, $CDCl_3$) δ (ppm): 181.6, 167.2, 154.1, 151.7, 145.3, 143.3, 133.1, 132.8, 131.2, 130.6, 129.8, 129.4, 128.8, 128.7, 125.2, 124.6, 108.9, 106.0, 102.8, 31.6, 31.5, 30.1, 29.3, 29.1,

28.9, 28.3, 28.2, 22.6, 22.5, 14.1. HRMS (ESI^+) m/z: found: $[M+H]^+$ 581.2535; molecular formula $C_{37}H_{41}O_2S_2$ requires $[M+H]^+$ 581.2542.

2.5.3. **(*E*)-5-(2-[5-(2,6-diphenyl-4*H*-pyran-4-ylidene)methyl)-3,4-dihexylthiophene-2-yl]vinyl)-3,4-dihexilthiophene-2-carbaldehyde (8)**

n-BuLi (1.6 M) in hexanes (0.8 mL, 1.26 mmol) was added to a solution of diphenyl(2,6-diphenyl-4*H*-pyran-4-yl) phosphine oxide (**11**) (0.502 g, 1.15 mmol) in dry THF (16 mL) at –30 ºC under argon atmosphere. The solution turned dark green and was stirred at this temperature for 15 min. Then, a solution of **12** (0.674 g, 1.15 mmol) in dry THF (10 mL) was slowly dropped, and the reaction was slowly warmed to room temperature for 24 h. A saturated solution of NH_4Cl (60 mL) was then added and the aqueous phase was extracted with CH_2Cl_2 (4×50 mL). The resulting organic layer was dried over $MgSO_4$ and evaporated. The crude product was purified by flash column chromatography (silicagel) with hexane/CH_2Cl_2 (1:1) as the eluent, to give **8** (0.364 g, 0.45 mmol, 40%) as a violet solid. Mp 127–129 ºC. IR (KBr) cm^{-1}: 1648 (C=O). ^{1}H-NMR (300 MHz, $CDCl_3$) δ (ppm): 9.97 (s, 1H), 7.93–7.72 (m, 4H), 7.52–7.40 (m, 6H), 7.31 (d, *J* = 15.4 Hz, 1H), 7.30 (d, *J* = 1.8 Hz, 1H), 6.93 (d, *J* = 15.4 Hz, 1H), 6.49 (d, *J* = 1.8 Hz, 1H), 6.06 (s, 1H), 2.93–2.80 (m, 2H), 2.69–2.51 (m, 6H), 1.67–1.48 (m, 8H), 1.47–1.28 (m, 24H), 0.98–0.79 (m, 12H). ^{13}C-NMR (100 MHz, $CDCl_3$) δ (ppm): 181.5, 153.1, 152.9, 150.7, 147.8, 143.2, 140.7, 140.3, 135.8, 134.1, 133.3, 132.9, 132.3, 129.3, 129.0, 128.5 (×2), 128.3, 124.9, 124.3, 123.9, 116.6, 109.1, 106.6, 103.2, 32.2, 31.6 (×2), 31.5, 31.4, 31.0, 30.8, 29.6, 29.5, 29.4 (×2), 29.3, 27.3, 27.2, 27.1, 26.4, 22.6 (×2), 22.5 (×2), 14.1, 14.0 (×2), 13.9. HRMS (ESI^+) m/z: found: $[M^{+\cdot}]$ 800.4598; molecular formula $C_{53}H_{68}O_2S_2$ requires $[M^{+\cdot}]$ 800.4652.

2.5.4. **2-cyano-3-(5-((2,6-diphenyl-4*H*-pyran-4-ylidene)methyl)thieno[3,2-*b*]thiophen-2-yl)acrylic acid (1a)**

To a solution of aldehyde **5a** (0.050 g, 0.12 mmol) and cyanoacetic acid (0.016 g, 0.19 mmol) in chloroform (2.5 mL), piperidine was added under argon atmosphere (80 μL, 0.8 mmol). The mixture was heated to reflux for 22 h, then cooled to 0 ºC. The resulting solid was isolated by filtration, washed with cold hexane, then with aqueous 0.1 M HCl and water, and finally dried. Product **1a** (0.036 g, 0.075 mmol, 62%) was obtained as a purple solid. Mp > 250 ºC (dec.). IR (KBr) cm^{-1}: 2210 (C≡N), 1650 (C=O), 1570 (C=C), 1552 (C=C). ^{1}H-NMR (400 MHz, DMSO-d_6) δ (ppm): 8.40 (s, 1H), 8.15 (s, 1H), 8.01–7.94 (m, 2H), 7.93–7.87 (m, 2H), 7.64–7.46 (m, 7H), 7.19 (s, 1H), 7.00 (s, 1H), 6.34 (s, 1H). ^{13}C-NMR (100 MHz, DMSO-d_6) δ (ppm): 162.4, 153.0, 152.5, 150.1, 147.1, 140.6, 137.5, 131.7, 131.6, 129.8, 129.2, 128.5, 126.8, 124.5, 123.9, 119.1, 117.0, 108.1, 107.7, 101.6. HRMS (MALDI^{+}) m/z: found: [$M^{+\cdot}$] 479.0631; molecular formula $C_{28}H_{18}NO_3S_2$ requires [$M^{+\cdot}$]: 479.0644; found: $[M+H]^+$ 480.0717; molecular formula $C_{28}H_{19}NO_3S_2$ requires $[M+H]^+$: 480.0723.

2.5.5. **2-cyano-3-(5-((2,6-di-*tert*-butyl-4*H*-pyran-4-ylidene)methyl)thieno[3,2-*b*]thiophen-2-yl)acrylic acid (1b)**

To a solution of aldehyde **5b** (0.070 g, 0.19 mmol) and cyanoacetic acid (0.024 g, 0.28 mmol) in chloroform (3 mL), piperidine was added under argon atmosphere (60 μL, 0.6 mmol). The mixture was heated to reflux for 22 h, and then cooled to 0 ºC. The resulting solid was isolated by filtration and washed with a cold mixture of hexane/dichloromethane 8:2, and then with aqueous 0.1 M HCl and water. Compound **1b** (0.031 g, 0.070 mmol, 38%) was obtained as a dark purple solid. Mp 174 ºC (dec.). IR (KBr) cm^{-1}: 2214 (C≡N), 1662 (C=O), 1550 (C=C). ^{1}H-NMR (400 MHz, DMSO-d_6) δ (ppm): 8.36 (s, 1H), 8.11 (s, 1H), 7.34 (s, 1H), 6.37 (s, 1H), 6.07 (s, 1H), 5.94 (s, 1H), 1.25 (s, 9H), 1.19 (s, 9H). ^{13}C-NMR (100 MHz,

THF-d_8): 166.6, 164.5, 163.9, 152.8, 148.6, 146.6, 137.8, 136.8, 133.3, 130.3, 117.0, 116.4, 105.9, 100.2, 97.7, 36.4, 35.9, 27.9 (×2). HRMS (ESI^+) m/z: found: $[M+H]^+$ 440.1348; molecular formula $C_{24}H_{26}NO_3S_2$ requires $[M+H]^+$ 440.1349; found: $[M+Na]^+$ 462.1164; molecular formula $C_{24}H_{25}NO_3S_2Na$ requires $[M+Na]^+$ 462.1168.

2.5.6. **(4*E*)-2-cyano-5-(5-((2,6-diphenyl-4*H*-pyran-4-ylidene)methyl)thieno[3,2-*b*]thiophen-2-yl)penta-2,4-dienoic acid (2)**

To a solution of aldehyde **6** (0.061 g, 0.14 mmol) and cyanoacetic acid (0.018 g, 0.21 mmol) in chloroform (3 mL), piperidine was added under argon atmosphere (90 μL, 0.91 mmol). The mixture was heated to reflux for 5 h, and then cooled to 0 ºC. The resulting solid was isolated by filtration, washed with a cold mixture of hexane/dichloromethane (8:2), then with aqueous 0.1 M HCl and water, and finally dried. Compound **2** (0.050 g, 0.099 mmol, 66%) was obtained as a purple solid. Mp 175–177 ºC. IR (KBr) cm^{-1}: 2214 (C≡N), 1652 (C=O), 1578 (C=C). ^{1}H-NMR (300 MHz, DMSO-d_6) δ (ppm): 8.44 (br s, 1H), 8.05–7.73 (m, 7H), 7.65–7.41 (m, 7H), 7.13 (s, 1H), 6.95 (s, 1H), 6.76 (dd, *J* = 14.7 Hz, *J'* = 11.8 Hz, 1H), 6.31 (s, 1H). ^{13}C-NMR: not registered due to low solubility. HRMS (ESI^-) m/z: found: $[M-H]^-$ 504.0721; molecular formula $C_{30}H_{18}NO_3S_2$ requires $[M-H]^-$ 504.0723.

2.5.7. **2-cyano-3-(5-((2,6-diphenyl-4*H*-pyran-4-ylidene)methyl)3,6-dihexylthieno[3,2-*b*]thiophen-2-yl)acrylic acid (3)**

To a solution of aldehyde **7** (0.045 g, 0.077 mmol) and cyanoacetic acid (0.011 g, 0.12 mmol) in chloroform (2.5 mL), piperidine was added under argon atmosphere (60 μL, 0.6 mmol). The mixture was heated to reflux for 96 h, and then cooled to 0 ºC. The resulting solid was isolated by filtration, washed with cold hexane, then with aqueous 0.1 M HCl and water, and finally dried. Compound **3** (0.020 g, 0.031 mmol, 42%) was obtained as a purple solid.

Mp 206–208 ºC. IR (KBr) cm^{-1}: 2212 (C≡N), 1652 (C=O), 1540 (C=C). ^{1}H-NMR (500 MHz, DMSO-d_6, 77 ºC, water presat.) δ (ppm): 8.30 (s, 1H), 7.93–7.86 (m, 4H), 7.61–7.45 (m, 6H), 7.20 (s, 1H), 7.03 (s, 1H), 6.39 (s, 1H), 3.00–2.90 (m, 2H), 2.85–2.75 (m, 1H), 1.78–1.63 (m, 4H), 1.43–1.24 (m, 12H), 0.91–0.81 (m, 6H). ^{13}C-NMR: not registered due to its low solubility. HRMS (ESI^+) m/z: found: $[M+H]^+$ 648.2607; molecular formula $C_{40}H_{42}NO_3S_2$ requires $[M+H]^+$ 648.2601.

2.5.8. **2-ciano-3-[5-(*E*)-2-(5-(2,6-diphenyl-4*H*-pyran-4-ylidene)methyl)-3,4-dihexylthiophene-2-yl)vinyl-3,4-dihexilthiophen-2-yl] acrylic acid.** (**4**)

To a solution of aldehyde **8** (0.116 g, 0.15 mmol) and cyanoacetic acid (0.019 g, 0.22 mmol) in chloroform (3 mL), piperidine was added under argon atmosphere (95 μL, 0.95 mmol). The mixture was heated to reflux for 72 h, then slowly cooled to room temperature, and acidified with 1M HCl. The organic layer was separated, washed with water and dried over $MgSO_4$. After removal of the solvent, the resulting solid was washed with hexane, then with a mixture hexane/CH_2Cl_2 (9:1) and dried. Compound **4** (0.082 g, 0.09 mmol, 65%) was obtained as a dark violet solid. Mp 224–229 ºC. IR (KBr) cm^{-1}: 2206 (C≡N), 1650 (C=O). ^{1}H-NMR (300 MHz, CD_2Cl_2) δ (ppm): 8.40 (s, 1H), 7.95–7.75 (m, 4H), 7.53–7.35 (m, 7H), 7.32 (d, *J* = 1.3 Hz, 1H), 7.02 (d, *J* = 15.4 Hz, 1H), 6.56 (d, *J* = 1.3 Hz, 1H), 6.12 (s, 1H), 2.82–2.52 (m, 8H), 1.54–1.27 (m, 32H), 0.95–0.81 (m, 12H). ^{13}C-NMR (100 MHz, CD_2Cl_2) δ (ppm): 156.9, 154.1, 151.5, 150.2, 145.1, 145.0, 141.5 (×2), 137.4, 133.8, 133.5, 133.3, 130.2, 129.8, 129.3 (×2), 128.6, 125.8, 125.6, 125.0, 117.2, 117.0, 109.8, 107.4, 103.7, 100.6, 93.2, 32.6, 32.3, 32.2, 32.1 (×2), 32.0, 31.5, 31.4, 30.3, 30.1, 30.0, 29.9, 28.2, 27.9, 27.8, 27.5, 23.3, 23.2, 23.1, 14.5, 14.4 (×3). HRMS (ESI^+) m/z: found: $[M^{+\cdot}]$ 867.4703; molecular formula $C_{56}H_{69}NO_3S_2$ requires $[M^{+\cdot}]$ 867.4713.

3. Results and discussion

3.1. Synthesis

Target dyes **1a–b**,**2–4** were prepared by Knoevenagel reaction of the 4*H*-pyranylidene-containing aldehydes **5a–b**,**6–8** and cyanoacetic acid in the presence of piperidine (Scheme 1). The resulting piperidinium salts, which precipitated in the reaction media (with the exception of **4**), were transformed into the corresponding pure products after the subsequent acid wash, in yields that ranged from 38 to 66%.

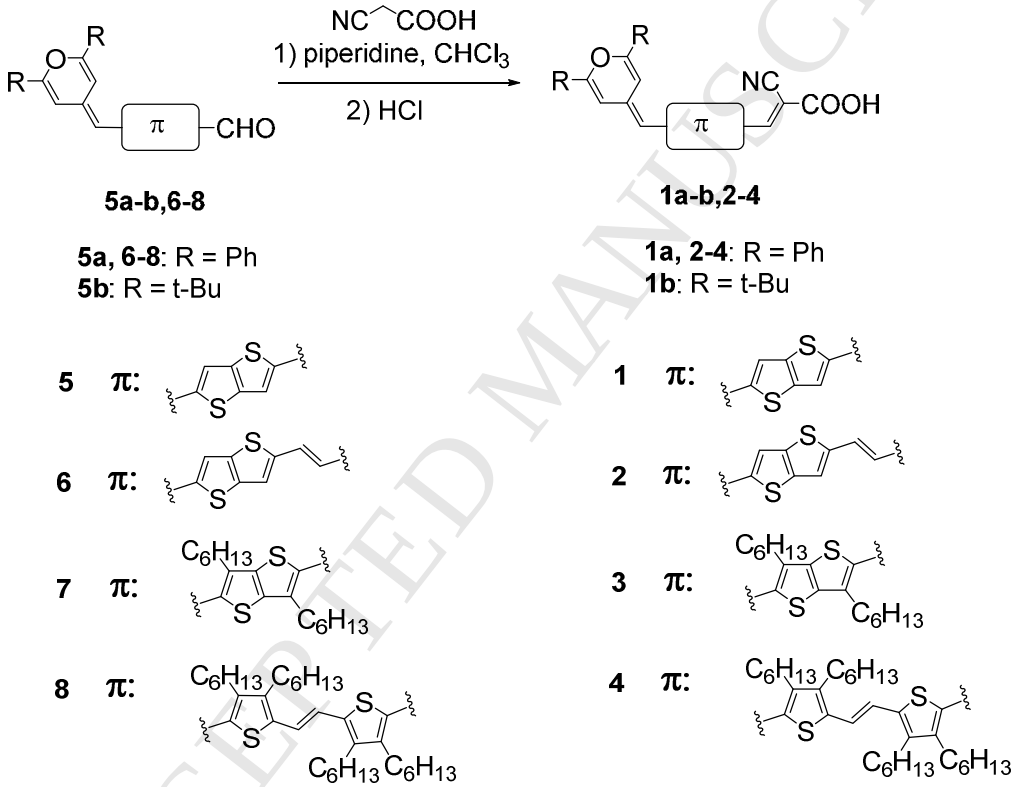

Scheme 1. Synthesis of 4*H*-pyranylidene-containing dyes **1a–b**,**2–4**.

Although compounds **5a–b**,**6** were obtained following described procedures (**5a,6:** [18b]; **5b:** [18c]), aldehydes **7** and **8** were unreported. These compounds were prepared according to the synthetic strategy depicted in Schemes 2 and 3, respectively.

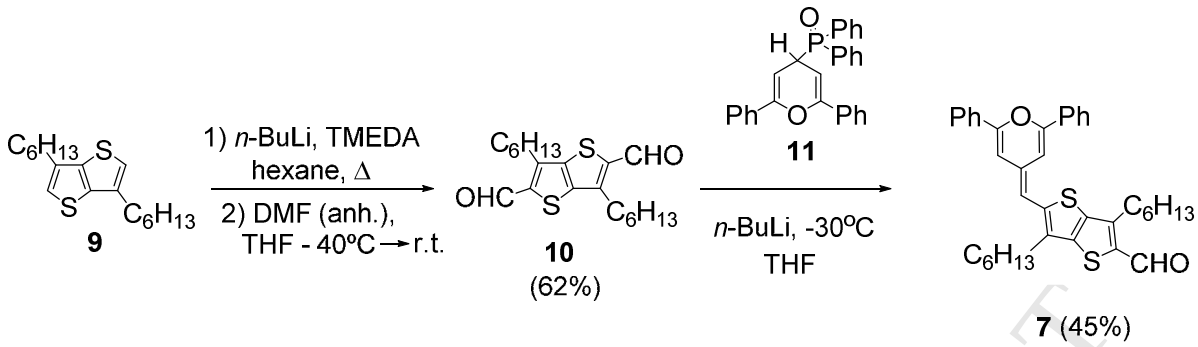

Scheme 2. Synthesis of aldehyde **7**.

Compound **7** was prepared from 3,6-dihexylthieno[3,2-*b*]thiophene **9**[29] in two steps. First, **10** was synthesized by reaction of DMF with the dilithiated derivative of **9**, formed in the presence of TMEDA (*N*,*N*,*N'*,*N'*-tetramethylethylendiamine).[22e,32] Next, a Horner reaction between 2,6-diphenyl-4*H*-pyran-4-yl)diphenylphosphine oxide (**11**)[30] and **10** afforded aldehyde **7**.

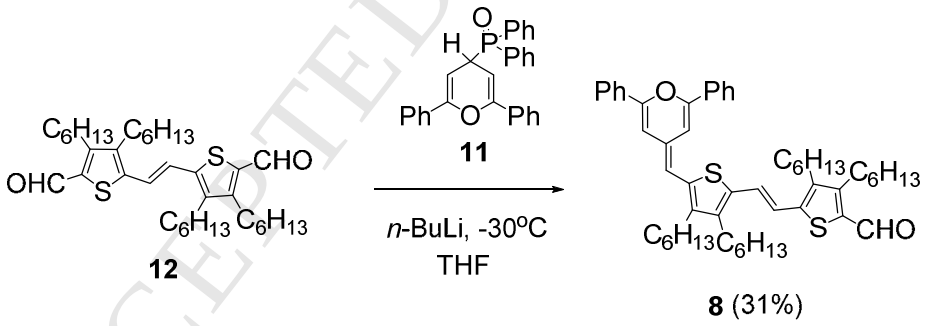

Scheme 3. Synthesis of aldehyde **8**.

Compound **8** was synthesized following a similar approach starting from the previously reported dialdehyde **12.**[31] It should be noted that the reaction conditions (temperature and order of slow addition of reagents) were carefully tuned in order to minimize the formation of pyranylidene-disubstituted derivatives as byproducts.[18b]

3.2. Optical properties

The photophysical properties of the synthesized dyes were examined by UV/vis and fluorescence spectroscopies in dichloromethane, and results are listed in Table 1.

Table 1: Optical properties.

Compd	λ_{abs}, nm (ε, M^{-1} cm^{-1})[a]	λ_{abs}, nm[b]	λ_{em}, nm[c]	Stokes shift, nm
1a	551 (21380)	464	655	104
1b	562 (28106)	478	647	85
2	583 (39811)	481	762	179
3	574 (44668)	496	706	132
4	626 (25119)	559	708	82

[a] Absorption maxima in CH_2Cl_2 solution. [b] Absorption maxima on TiO_2 films (3μm thick). [c] In CH_2Cl_2 solution. Dyes were excited at the wavelength of maximum absorption.

All dyes exhibit intense and broad bands in the visible region, which can be assigned to an ICT process between the donor and the acceptor. (See spectra in the Supporting Information) Molar extinction coefficients (ε) obtained for compounds **1a–b**,**2–4** range from 21380 to 44660 $M^{-1}cm^{-1}$, exceeding those of the standard ruthenium dyes **N3**[33] and **N719**[34] (13900 and 14000 $M^{-1}cm^{-1}$, respectively), and pointing to this series of compounds as good candidates for light harvesting.

A relationship between the energy of the ICT band and the π-relay can be inferred from data in Table 1. Concerning TT derivatives (**1a–b**, **2–3**), a bathochromic effect is observed on replacing phenyl rings for *tert*-butyl groups on the pyran moiety (**1b**), on lengthening the π-spacer (**2**), and upon the introduction of hexyl substituents on the TT ring (**3**). Compound **4**, with the largest π-conjugation path presents the highest λ_{abs} value, extending its absorbance until near 800 nm.

Attaching dyes to TiO_2 surface (Figure 2) causes a significant blue shift of λ_{abs} (in some cases, as **2**, close to 100 nm) when compared to CH_2Cl_2 solutions. This hypsochromic shift was accompanied by a considerable broadening of the absorption band, indicating strong interactions between the dyes and the semiconductor surface.[28] These blue-shifted values may be attributed to the deprotonation of carboxylic acid upon adsorption onto the TiO_2 surface, with the resulting carboxylate-TiO_2 unit a weaker electron acceptor compared to the carboxylic acid.[35] They have been reported for other organic dyes on TiO_2 electrodes.[16b,20g,25a]

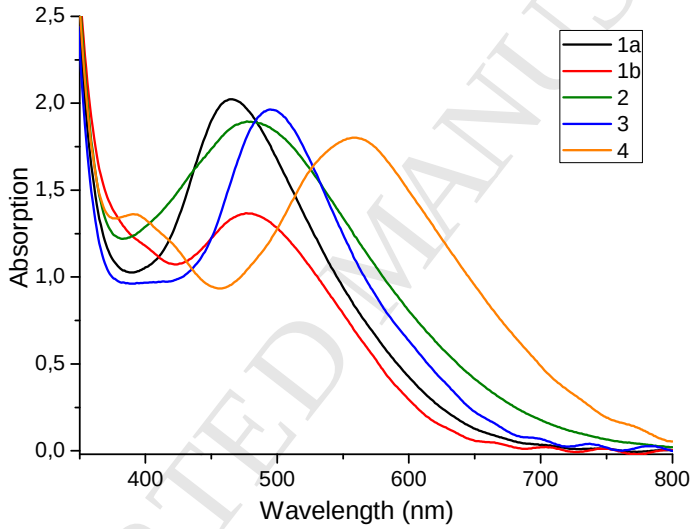

Fig. 2. Absorption spectra of studied organic dyes on TiO_2 transparent films.

With respect to the fluorescence features, low-intensity bands were observed for all compounds, together with large Stokes shifts. Emission spectra allowed the determination of the $E_{0\text{-}0}$ (zeroth-zeroth transition energy) for all dyes. (See Table 2 in 3.3. Electrochemical properties section)

3.3. Electrochemical study

In order to evaluate the processes of electron transfer from the excited dye molecules to the conduction band of TiO_2 and the subsequent regeneration of the oxidized dye, the electrochemical properties of dyes adsorbed on TiO_2 films (after 2 h immersion in CH_2Cl_2 10^{-4} M solution) were studied by using differential pulse voltammetry (DPV) methods. Data are collected in Table 2, together with the estimated excited-state oxidation potentials.

Table 2: Electrochemical data.

Compd	E_{ox} [a] (V) (vs NHE)	$E_{0\text{-}0}$ [b] (eV)	E_{ox}* [c] (V) (vs NHE)
1a	0.70	2.00	−1.30
1b	0.76	2.01	−1.25
2	0.70	1.88	−1.18
3	0.71	1.96	−1.25
4	0.62	1.82	−1.20

[a] The oxidation potentials, measured in CH_2Cl_2 with 0.1 M $TBAPF_6$ as electrolyte, Ag/AgCl as reference electrode and Pt as counter electrode respectively, were converted to normal electrode (NHE) by addition of 0.199 V. [b] Zeroth-zeroth transition energy estimated from the intersection of normalized absorption and emission spectrum in CH_2Cl_2 solution. [c] Excited-state oxidation potential obtained from $E_{ox} - E_{0\text{-}0}$.

Ground-state oxidation potentials higher than the redox potential of the iodide/triiodide couple (+0.42 V vs NHE)[36] were found in all cases, ensuring in such a way the regeneration of the oxidized form of the dye. The nature of the heteroaromatic ring used as π-spacer was found to affect significantly the oxidation potential values. Thus, TT derivatives (**1a–b**, **2–3**) show E_{ox} values higher than compound **4**, indicating a more efficient electron transfer from the I^- to the oxidized dyes for the former family. This observed trend is also confirmed by

computational calculations (Table 3; section 3.4.), which show lower E_{HOMO} values for TT series.

Concerning TT systems, and taking compound **1a** as model, adding an ethylenic unit (**2**) or introducing hexyl chains (**3**) does not imply a variation on the E_{ox} value. Nevertheless, there is a shift towards an increasingly anodic potential when passing from **1a** (with phenyl groups in the 4*H*-pyranylidene unit) to **1b** (with *tert*-butyl ones), in agreement with other 4*H*-pyranylidene-based dyes for DSSCs bearing phenyl or *tert*-butyl substituents in 2,6 positions.[15a,25c]

The excited state potential (E_{ox}*) was deduced from the expression $E_{ox} - E_{0\text{-}0}$, where $E_{0\text{-}0}$ energies were estimated from the intercept of the normalized absorption and emission spectra (Tables 1 and 2). All E_{ox}* values are far more negative than the energy of the conduction band gap edge of TiO_2 (−0.5 V vs NHE),[36] required for the electron injection process from the excited dyes to the TiO_2 conduction band to be efficient.

3.4. Theoretical calculations

In order to get further insight in the electronic and optical properties of the studied compounds, theoretical calculations using TD-DFT (Time Dependent Density Functional Theory) and the CPCM (Conductor-like Polarizable Continuum Model) solvation method were performed.

Calculations at the ground state geometry allowed to obtain orbital energies and topologies, and absorption wavelengths (λ_{abs}). The first excited state geometries were optimized in order to obtain the emission wavelength (λ_{em}) and estimate $E_{0\text{-}0}$ values, which were approached to adiabatic excitation energies to avoid the large computational cost required to compute excited state vibrational energies. Calculations were also performed on the oxidized radical cations in order to obtain the oxidation potentials of the studied compounds on both their ground and first excited states. All data are collected in Table 3.

Table 3. Results of DFT calculations[a] for studied dyes.

Compd	λ_{abs}, nm	E_{HOMO} (eV)	E_{LUMO} (eV)	λ_{em}, nm	$E_{0\text{-}0}$ (eV)	E_{ox} *(V) (vs* NHE*)*	Eox^{*} *(V) (vs* NHE*)*
1a	551	−6.31	−2.34	684	1.99	0.82	−1.18
1b	537	−6.27	−2.22	644	2.19	0.82	−1.27
2	569	−6.21	−2.40	762	1.86	0.81	−1.05
3	556	−6.24	−2.29	706	1.96	0.89	−1.07
4	618	−5.96	−2.35	910	1.64	0.58	−1.06

[a] Calculated at the CPCM-M06-2X/6-311+G(2d,p)//M06-2X/6-31G* level in CH_2Cl_2.

Compared to experimental results and concerning λ_{abs}, theoretical calculations provide a reasonable accuracy, with a mean absolute error of 25 nm (0.10 eV) for derivative **1b**, and reproduce the experimental trends discussed in section 3.2.

It can be seen that there is a reasonably good agreement between calculated and experimental results shown in Tables 1 and 2, respectively, for TT derivatives. However, calculations do not reproduce experimental data for system **4**, particularly in the wavelength emission.

According to the calculations, electron densities related to frontier orbitals (see topologies for compound **1b** in Figure 3) are mainly supported by the 4*H*-pyranylidene unit and its adjacent thienyl ring for the HOMO, and by the cyanoacrylic acid fragment and its nearest thiophene unit in the case of LUMO. These results are in agreement with those found for other D–A compounds featuring a TT relay in their structure.[22e] Moreover, the first excited state is mainly contributed from a one electron HOMO to LUMO transition, and there is a large HOMO-LUMO spatial overlap that accounts for the high molar extinction coefficients (ε).

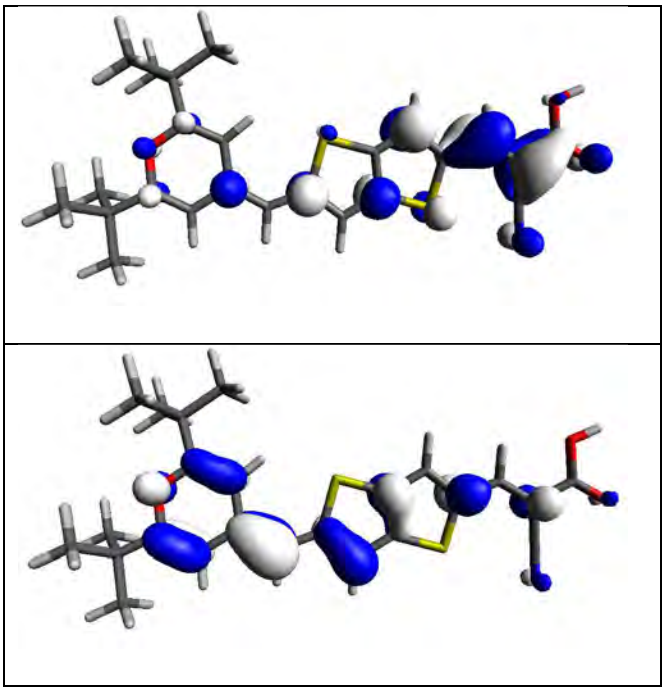

Fig. 3. Illustration of the HOMO (bottom) and LUMO (top) of compound **1b**.

Concerning the geometrical configuration of the studied dyes, in the ground state, the π-system of all compounds is almost planar. For compounds **1a**, **2−4**, the dihedral angles between the 4*H*-pyranylidene moiety and the two phenyl rings connected in its 2,6 positions were near to 20º (See Figure S-23, for compound **2**), in agreement with the X-ray structure of a conjugated ferrocenyl methylenepyran derivative with phenyl substituents in positions 2,6.[37] These two phenyl rings may help to suppress dye aggregation when dyes **1a**, **2−4** are loaded on TiO_2 films.[20g]

On the basis of the spin density plots calculated for the oxidized radical cations corresponding to compounds **1−4**, it can be seen that most of the spin density (the hole) spreads (see Figure 4 for compound **1b**) on the *4H*-pyranylidene donor and the heterocyclic spacer, making difficult the back electron transfer (BET) from the TiO_2 electrode. There is, however, some spin density on the cyanoacetic acceptor linked to the electrode and therefore BET cannot be completely excluded.

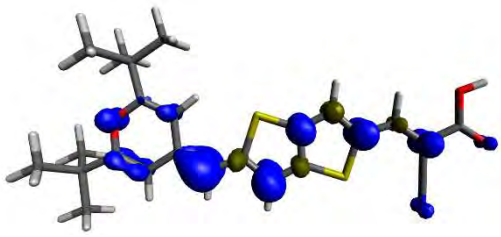

Fig. 4. Spin density plot of radical cation of compound **1b**.

3.5. Photovoltaic properties

According to previous studies carried out in our research group[25f] the photovoltaic properties of the sensitizers were studied, defining the optimized conditions as 0.1 mM for the dye and 0.3 mM for chenodeoxycolic acid in anhydrous CH_2Cl_2, and an electrolyte based on the classical I^-/I_3^- system (1-butyl-3-methylimidazolium iodide (0.53 M), LiI (0.10 M), I_2 (0.050 M) and *tert*-butylpyridine (0.52 M) in anhydrous acetonitrile). The thickness of photoanodes prepared from commercial Dyesol® 18NR-AO was measured to be 15 μm with an effective area of 0.25 cm^2. The devices were prepared after 6 h of immersion of the electrodes in the corresponding dye solutions.

The relevant photovoltaic parameters, the open circuit voltage (V_{oc}), the short circuit current (J_{sc}), the fill factor (*ff*), and solar-to-electrical energy conversion efficiencies (η) are collected in Table 4. Moreover, current density-voltage (*J*-*V*) curves and incident photon- to- current conversion efficiencies (IPCE) of devices based on these dyes are represented in Figures 5 and 6, respectively.

Table 4. Photovoltaic properties of DSSCs constructed using the dyes **1a–b**, **2–4.**

Compd	J_{sc} (mA cm^{-2})	V_{oc} (V)	*ff* (%)	η (%)	τ_n (ms)
1a	13.51	0.519	59.0	4.13	0.79
1b	16.94	0.569	62.8	6.06	3.22
2	10.05	0.475	56.2	2.68	0.59
3	16.82	0.592	64.4	6.41	2.43
4	12.30	0.571	63.5	4.45	5.66

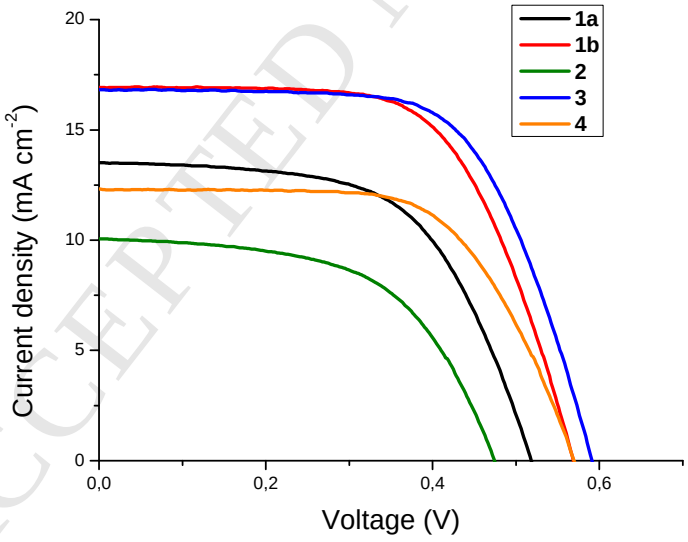

Fig. 5. *J-V* curves recorded under AM 1.5 G illumination for DSSC devices.

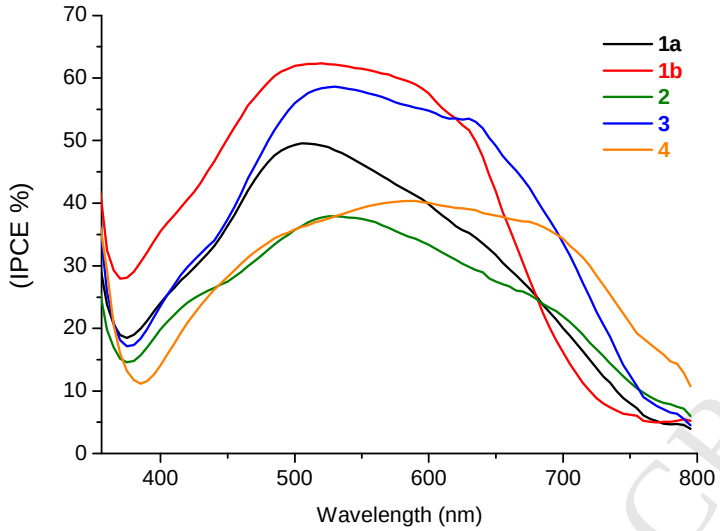

Fig. 6. IPCE spectra of devices prepared from studied dyes.

Higher values for power conversion efficiency (η) have been encountered for TT derivatives **1b** and **3**. In this series, the replacement of phenyl group (**1a**) by *tert*-butyl side group (**1b**) in the 4*H*-pyranylidene ring and the modification of the thienothiophene with two hexyl groups (**3**) results in higher values of J_{sc} and V_{oc} parameters, and, thus, in a significant increase in the efficiency value. The enhanced V_{oc} for compound **3** may be attributed to the suppression of the intermolecular π-π aggregation and the electron recombination by the hexyl chains attached to the TT linker.[20f,i] Nevertheless, lengthening the π-spacer with an ethylenic fragment (compound **2**) does not lead to an improvement of the performance of the final DSSC,[38] being J_{sc}, V_{oc} and *ff* values worse than those for **1a**.

Devices prepared from dye **4** showed a better performance than those prepared from **1a** and **2**, due to its higher V_{oc} value. However, the incorporation of four hexyl chains neither does improve the results obtained with compound **1b**, indicating that the rigid TT spacer plays an important role in the studied dyes, favoring the injection of electrons in the photoanode, as manifested in its higher J_{sc} value.

To the best of our knowledge, the value of 6.41% measured for system **3** represents the highest efficiency ever reported for a DSSC based on an organic sensitizer with a 4*H*-pyranylidene as electron donor fragment.

In terms of IPCE tendencies, for TT derivatives, and taking system **1a** as model compound, the introduction of two hexyl groups in the TT ring (dye **3**) allows expanding the spectral window until 800 nm, with a maximum and nearly constant photoresponse in the range 500–650 nm (maximum 58%). On the other hand, the replacement of phenyl groups by *tert*-butyl ones in the pyranylidene ring (dye **1b**) results in a higher IPCE maximum (63%), but in the range 450–600 nm. The observed IPCE values lead to similar J_{sc} values for these sensitizers, higher than that of the parent **1a**. The IPCE for compound **2** displayed the poorest performance with the lowest IPCE values, data consistent with the lowest J_{sc} value. Finally, it can be observed that for compound **4** the IPCE spectrum is broadened at higher wavelengths, but with a maximum of only 40%, indicating that with this compound injection of electrons is less favored.

Electrochemical impedance spectroscopy (EIS) is a dynamic technique to study the electron transport kinetics and photoelectrochemical processes in DSSCs devices. The EIS measurements were carried out under AM 1.5 G simulated solar light (100 mW cm^{-2}) at open circuit voltage conditions. Bode phase plots (Figure 7) were used to estimate the lifetime of electrons (τ) in the conduction band of TiO_2.[39,40] The τ values gathered in Table 4 were calculated using the equation: $\tau = 1/2\ \pi f$ where *f* stands for the frequency at the maximum of the curve in the intermediate frequency region in the Bode plot.

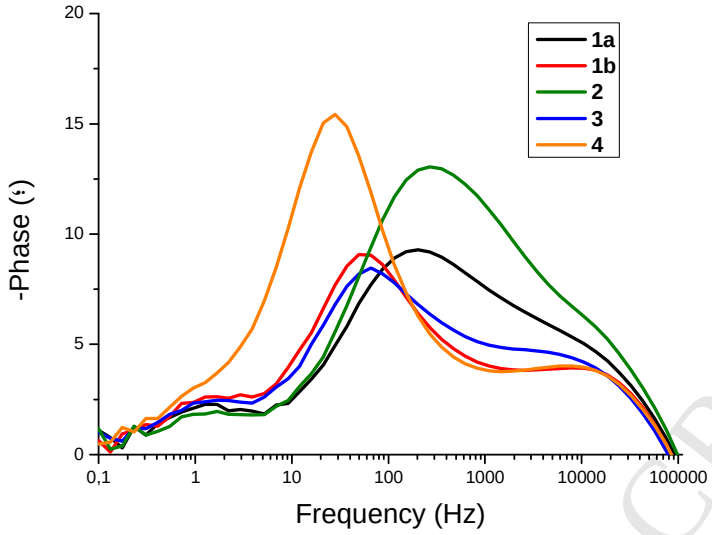

Fig. 7.- Bode phase plots of compounds studied obtained by EIS.

The order of lifetimes encountered is **4**>**1b**>**3**>**1a**>**2**, and supports the fact that devices based on compounds **1a**, **2** present the lowest V_{oc} values along the studied series, probably because the recombination processes are favored in these compounds. Thereby, either the presence of hexyl substituents in the heterocyclic rings or the *tert*-butyl groups in 2,6 positions of the pyranylidene unit, lead to a reduction of the recombination processes on the TiO_2 surface. The bode plots results are in agreement with the experimental *J*-*V* curves.

4. Conclusions

We have designed and synthesized four efficient sensitizers containing a 4*H*-pyranylidene moiety as donor and a TT unit in the π-spacer. The photovoltaic performance was shown to be sensitive to the substituents on the sensitizers: the replacement of the phenyl group by a *tert*-butyl one in the pyran unit and the inclusion of hexyl chains in the TT core lead to an increase in the efficiency value. The efficiency data for dye **3** (6.41%), with a dihexylthieno[3,2-*b*]thiophene relay represents the highest performance ever reported for a DSSC based on the 4*H*-pyranylidene unit as donor end.

Acknowledgments. Financial support from MINECO (CTQ2014-52331R) and Gobierno de Aragón-FEDER-Fondo Social Europeo 2014–2020 (E14_17R) is gratefully acknowledged. A predoctoral fellowship to A. B. Marco (FPI BES–2009–016966) is also acknowledged.

References

[1] a) Huang Y, Kramer EJ, Heeger AJ, Bazan GC. Bulk heterojunction solar cells: morphology and performance relationships. Chem Rev 2014;114:7006–43; b) Ragoussi M-E, Torres T. New generation solar cells: concepts, trends and perspectives. Chem Commun 2015;51:3957–72.

[2] a) Hagfeldt A, Boschloo G, Sun L, Kloo L, Pettersson H. Dye-sensitized solar cells. Chem Rev 2010;110:6595–663; b) Hardin BE, Snaith HJ, McGehee MD. The renaissance of dye-sensitized solar cells. Nat Phot 2012;6:162–9.

[3] See for example: a) Nazeeruddin MK, De Angelis F, Fantacci S, Selloni A, Viscardi G, Liska, P et al. Combined experimental and DFT-TDDFT computational study of photoelectrochemical cell ruthenium sensitizers. J Am Chem Soc 2005;127:16835−47; b) Chiba Y, Islam A, Watanabe Y, Komiya R, Koide N, Han L. Dye-sensitized solar cells with conversion efficiency of 11.1%. Jpn J Appl Phys 2006;45:L638−40.

[4] Bignozzi CA, Argazzi R, Boaretto R, Busatto E, Carli S, Ronconi F et al. The role of transition metal complexes in dye sensitized solar devices. Coord Chem Rev 2013;257:1472–92.

[5] Kakiage K, Aoyama Y, Yano T, Oya K, Fujisawa J-i, Hanaya M. Highly-efficient dye-sensitized solar cells with collaborative sensitization by silyl-anchor and carboxy-anchor dyes. Chem Commun 2015;51:15894–7.

[6] a) Srinivas K, Yesudas K, Bhanuprakash K, Rao VJ, Giribabu L. Combined experimental and computational investigation of anthracene based sensitizers for DSSC:

comparison of cyanoacrylic and malonic acid electron withdrawing groups binding onto the TiO_2 anatase (101) surface. J Phys Chem C 2009;113:20117–26; b) Wiberg J, Marinado T, Hagberg DP, Sun L, Hagfeldt A, Albinsson B. Effect of anchoring group on electron injection and recombination dynamics in organic dye-sensitized solar cells. J Phys Chem C 2009;113:3881–6.

[7] Review: Wang J, Liu K, Ma L, Zhan, X. Triarylamine: versatile platform for organic, dye-sensitized, and perovskite solar cells. Chem Rev 2016;116:14675–725.

[8] Liang M, Chen J. Arylamine organic dyes for dye-sensitized solar cells. Chem Soc Rev 2013;42:3453–88.

[9] a) Yang J, Ganesan P, Teuscher J, Moehl T, Kim YJ, Yi C et al. Influence of the donor size in D-π-A organic dyes for dye-sensitized solar cells. J Am Chem Soc 2014;136:5722–30; b) Alagumalai A, Fairoos M.K. M, Vellimalai P, Chandra Sil M, Nithyanandhan J. Effect of out-of-plane alkyl group's position in dye-sensitized solar cell efficiency: a structure−property relationship utilizing indoline-based unsymmetrical squaraine dyes. ACS Appl Mater Interfaces 2016;8:35353–67.

[10] a) Soni SS, Fadadu KB, Vaghasiya JV, Solanki, BG, Sonigara KK, Singh A et al. Improved molecular architecture of D–π–A carbazole dyes: 9% PCE with a cobalt redox shuttle in dye sensitized solar cells. J Mater Chem A 2015;3:21664–71; b) Sathiyan G, Sivakumar EKT, Ganesamoorthy R, Thangamuthu R, Sakthivel P. Review of carbazole based conjugated molecules for highly efficient organic solar cell application. Tetrahedron Lett 2016;57:243–252.

[11] a) Wan Z, Jia C, Duan Y, Chen X, Li Z, Lin Y. Novel organic sensitizers containing dithiafulvenyl units as additional donors for efficient dye-sensitized solar cells. RSC Adv 2014;4:34896–903; b) Luo J, Wan Z, Jia C, Wang Y, Wu X, Yao X. Co-sensitization of

Dithiafulvenyl-Phenothiazine Based Organic Dyes with N719 for Efficient Dye-Sensitized Solar Cells. Electrochimica Acta 2016;211:364–74.

[12] a) Wenger S, Bouit P-A, Chen Q, Teuscher J, Di Censo D, Humphry-Baker R, Moser J-E, Delgado JL, Martín N, Zakeeruddin SM, Grätzel M. Efficient electron transfer and sensitizer regeneration in stable π-extended tetrathiafulvalene-sensitized solar cells. J Am Chem Soc 2010;132:5164–9; b) Brunetti FG, López JL, Atienza C, Martín N. π-Extended TTF: a versatile molecule for organic electronics. J Mater Chem 2012;22:4188–205.

[13] a) Gao P, Tsao HN, Yi C, Grätzel M, Nazeeruddin MK. Extended π-bridge in organic dye-sensitized solar cells: the longer, the better? Adv Energy Mater 2014;4:1301485–91; b) Paramasivarn M, Chitumalla RK, Singh SP, Islam A, Han L, Rao VJ et al. Tuning the photovoltaic performance of benzocarbazole-based sensitizers for dyesensitized solar cells: a joint experimental and theoretical study of the influence of π-spacers. J Phys Chem C 2015;119:17053–64.

[14] a) Li R, Lv X, Shi D, Zhou D, Cheng Y, Zhang G et al. Dye-sensitized solar cells based on organic sensitizers with different conjugated linkers: furan, bifuran, thiophene, bithiophene, selenophene, and biselenophene. J Phys Chem C 2009;113:7469–79; b) Seo KD, Choi IT, Kim HK. Organic dyes with well-defined structures for highly efficient dye-sensitized solar cells based on a cobalt electrolyte. Chem Eur J 2015;21:14804–11.

[15] a) Pérez-Tejada R, Pellejà L, Palomares E, Franco S, Orduna J, Garín J et al. Novel 4*H*-pyranylidene organic dyes for dye-sensitized solar cells: effect of different heteroaromatic rings on the photovoltaic properties. Org Electron 2014;15:3237–50; b) Dessi A, Calamante M, Mordini A, Peruzzini M, Sinicropi A, Basosi R et al. Organic dyes with intense light absorption especially suitable for application in thin-layer dye-sensitized solar cells. Chem Commun 2014;50:13952–5.

[16] a) Zhou H, Yang L, Stuart AC, Price SC, Liu S, You W. Development of fluorinated benzothiadiazole as a structural unit for a polymer solar cell of 7 % efficiency. Angew Chem Int Ed 2011;50:2995–8; b) Duerto I, Colom E, Andrés-Castán JM, Franco S, Garín J, Orduna J et al. DSSCs based on aniline derivatives functionalized with a tert-butyldimethylsilyl group and the effect of the π-spacer. Dyes Pigm. 2018;148:61–71.

[17] Reviews: a) Litvinov VP. The chemistry of thienothiophenes. Adv Heterocycl Chem 2006;90:125–203; b) Cinar ME, Ozturk T. Thienothiophenes, dithienothiophenes, and thienoacenes: syntheses, oligomers, polymers, and properties. Chem Rev 2015;115:3036–40.

[18] Selected examples: a) Rao VP, Wong KY, Jen AK-Y, Drost KJ. Functionalized fused thiophenes: a new class of thermally stable and efficient second-order nonlinear optical chromophores. Chem Mater 1994;6:2210–2; b) Marco AB, Andreu R, Franco S, Garín J, Orduna J, Villacampa B et al. Efficient second-order nonlinear optical chromophores based on dithienothiophene and thienothiophene bridges. Tetrahedron 2013;69:3919–26; c) Marco AB, Andreu R, Franco S, Garín J, Orduna J, Villacampa B et al. Push–pull systems bearing a quinoid/aromatic thieno-[3,2-b]thiophene moiety: synthesis, ground state polarization and second-order nonlinear properties. Org Biomol Chem 2013;11:6338–49; d) Raposo MMM, Herbivo C, Hugues V, Clermont G, Castro MCR, Comel A et al. Synthesis, fluorescence, and two-photon absorption properties of push–pull 5-arylthieno[3,2-*b*]thiophene derivatives. Eur J Org Chem 2016;5263–73.

[19] Gather MC, Heeney M, Zhang W, Whitehead KS, Bradley DDC, McCulloch I et al. An alignable fluorene thienothiophene copolymer with deep-blue electroluminescent emission at 410 nm. Chem Commun 2008;1079–81.

[20] Selected examples: a) Li S-L, Jiang K-J, Shao K-F, Yang L-M. Novel organic dyes for efficient dye-sensitized solar cells. Chem Commun 2006;2792–4; b) Li G, Jiang K-J, Li Y-F, Li S-L, Yang L-M. Efficient structural modification of triphenylamine-based organic dyes for

dye-sensitized solar cells. J Phys Chem C 2008; 112:11591–9; c) Xu M, Li R, Pootrakulchote N, Shi D, Guo J, Yi Z et al. Energy-level and molecular engineering of organic D-π-A sensitizers in dye-sensitized solar cells. J Phys Chem C 2008;112:19770–6; d) Zhang G, Bala H, Cheng Y, Shi D, Lv X, Yu Q et al. High efficiency and stable dye-sensitized solar cells with an organic chromophore featuring a binary π-conjugated spacer. Chem Commun 2009;2198–200; e) Paek S, Choi H, Choi H, Lee C-W, Kang M-s, Song K et al. Molecular engineering of efficient organic sensitizers incorporating a binary π-conjugated linker unit for dye-sensitized solar cells. J Phys Chem C 2010;114:14646–53; f) Kim D, Kim C, Choi H, Song K, Kang M-S, Ko J. A new class of organic sensitizers with fused planar triphenylamine for nanocrystalline dye sensitized solar cells J Photochem Photobiol A 2011;219:122–31; g) Cai S, Tian G, Li X, Su J, Tian H. Efficient and stable DSSC sensitizers based on substituted dihydroindolo[2,3-b]carbazole donors with high molar extinction coefficients. J Mater Chem A 2013;1:11295–305; h) Lee M-W, Kim J-Y, Lee D-H, Ko MJ. Novel D□π□A organic dyes with thieno[3,2-b]thiophene-3,4-ethylenedioxythiophene unit as a π□bridge for highly efficient dye-sensitized solar cells with long-term stability. ACS Appl Mater Interfaces 2014;6:4102–8; i) Zhu S, An Z, Chen X, Chen P, Liu Q. Cyclic thiourea functionalized dyes with binary π-linkers: Influence of different π-conjugation segments on the performance of dye-sensitized solar cells. Dyes Pigm 2015;116:146–54; j) Fernandes SSM, Castro MCR, Mesquita I, Andrade L, Mendes A, Raposo MMM. Synthesis and characterization of novel thieno[3,2-b]thiophene based metal-free organic dyes with different heteroaromatic donor moieties as sensitizers for dye-sensitized solar cells. Dyes Pigm 2017;136:46–53; k) Eom YK, Hong JY, Kim J, Kim HK. Triphenylamine-based organic sensitizers with π-spacer structural engineering for dye-sensitized solar cells: synthesis, theoretical calculations, molecular spectroscopy and structure-property performance relationships. Dyes Pigm 2017;136:496–504.

[21] Andreu R, Carrasquer L, Franco S, Garín J, Orduna J, Martínez de Baroja N et al. 4*H*-Pyran-4-ylidenes: strong proaromatic donors for organic nonlinear optical chromophores. J Org Chem 2009;74:6647–57.

[22] Selected examples for 4*H*-pyranylidene-containing chromophores: a) Faux N, Caro B, Robin-le Guen F, Le Poul P, Nakatani K, Ishow E. γ-Methylene chalcogenapyrans and benzopyrans as proaromatic donors in ‘‘push–pull’’ Fischer type carbine complexes: Influences of chalcogen atom and chain length on the electronic and N.L.O. properties of these molecules. J Organomet Chem 2005;690:4982−8; b) Andreu R, Galán E, Orduna J, Villacampa B, Alicante R, López Navarrete JT et al. Aromatic/proaromatic donors in 2-dicyanomethylenethiazole merocyanines: from neutral to strongly zwitterionic nonlinear optical chromophores. Chem Eur J 2011;17:826–38; c) Martínez de Baroja N, Garín J, Orduna J, Andreu R, Blesa MJ, Villacampa B et al. Synthesis, characterization, and optical properties of 4H-pyran-4-ylidene donor-based chromophores: the relevance of the location of a thiophene ring in the spacer. J Org Chem 2012;77:4634–44; d) Achelle S, Malval J-P, Aloïse S, Barsella A, Spangenberg A, Mager L et al. Synthesis, photophysics and nonlinear optical properties of stilbenoid pyrimidine-based dyes bearing methylenepyran donor groups. ChemPhysChem 2013;14:2725−36; e) Marco AB, Martínez de Baroja N, Franco S, Garín J, Orduna J, Villacampa B et al. Dithienopyrrole as a rigid alternative to the bithiophene π-relay in chromophores with second-order nonlinear optical properties. Chem Asian J 2015;10:188−97; f) Moreno-Yruela C, Garín J, Orduna J, Franco S, Quintero E, López Navarrete JT et al. D-π-A compounds with tunable intramolecular charge transfer achieved by incorporation of butenolide nitriles as acceptor moieties. J Org Chem 2015;80:12115–28; g) Solanke P, Achelle S, Cabon N, Pytela O, Barsella A, Caro B et al. Proaromatic pyranylidene chalcogen analogues and cyclopenta[c]thiophen-4,6-dione as electron donors and acceptor in efficient charge-transfer chromophores. Dyes Pigm 2016;134:129–38; h) Durand RJ, Gauthier S,

Achelle S, Groizard T, Kahlal S, Saillard J-Y et al. Push–pull D–π-Ru–π-A chromophores: synthesis and electrochemical, photophysical and secondorder nonlinear optical properties. Dalton Trans 2018;47:3965–75.

[23] a) Ambrosio A, Orabona E, Maddalena P, Camposeo A, Polo M, Neves AAR et al. Two-photon patterning of a polymer containing Y-shaped azochromophores. Appl Phys Lett 2009;94:011115; b) Ambrosio A, Maddalena P, Carella A, Borbone F, Roviello A, Polo M, et al. Two-Photon induced self-structuring of polymeric films based on Y-shape azobenzene chromophore. J Phys Chem C 2011;28:13566–70; c) Poronik YM, Hugues V, Blanchard-Desce M, Gryko DT. Octupolar merocyanine dyes: a new class of nonlinear optical chromophores. Chem Eur J 2012;18:9258–66.

[24] a) Xue J, He J, Gu X, Yang Z, Xu B, Tian W. Efficient bulk-heterojunction solar cells based on a symmetrical D-π-A-π-D organic dye molecule. J Phys Chem C 2009;113:12911–7; b) Li Z, Dong Q, Xu B, Li H, Wen S, Pei J et al. New amorphous small molecules-Synthesis, characterization and their application in bulk heterojunction solar cells. Sol Energy Mater Sol Cells 2011;95:2272–80.

[25] Selected examples: a) Bolag A, Nishida J-i, Hara K, Yamashita Y. Dye-sensitized solar cells based on novel diphenylpyran derivatives. Chem Lett 2011;40:510–1; b) Bolag A, Nishida J-i, Hara K, Yamashita Y. Enhanced performance of dye-sensitized solar cells with novel 2,6-diphenyl-4H-pyranylidene dyes. Org Electron 2012;13:425–31; c) Franco S, Garín J, Martínez de Baroja N, Pérez-Tejada R, Orduna J, Yu Y et al. New D-π-A-conjugated organic sensitizers based on 4H-pyran-4-ylidene donors for highly efficient dye-sensitized solar cells. Org Lett 2012;14:752–5; d) Sharma GD, Patel KR, Roy MS, Misra R. Characterization of two new $(A–\pi)_2$–D–A type dyes with different central D unit and their application for dye sensitized solar cells. Org Lett 2014;15:1780–90; e) Pérez-Tejada R, Martínez de Baroja N, Franco S, Pellejà L, Orduna J, Andreu R et al. Organic sensitizers

bearing a trialkylsilyl ether group for liquid dye sensitized solar cells. Dyes Pigm 2015;123:293–303; f) Andrés-Castán JM, Franco S, Villacampa B, Orduna J, Pérez-Tejada R. New efficient tert-butyldiphenyl-4H-pyranylidene sensitizers for DSSCs. RSC Adv 2015;5:106706–9.

[26] Awuaha SG, Polreis J, Prakash J, Qiao Q, You Y. New pyran dyes for dye-sensitized solar cells. J Photochem Photobiol A 2011;224:116–22.

[27] a) Maglione C, Carella A, Centore R, Fusco S, Velardo A, Peluso A et al. Tuning optical absorption in pyran derivatives for DSSC. J Photochem Photobiol A 2016;321:79–89; b) Maglione C, Carella A, Carbonara C, Centore R, Fusco S, Velardo A et al. Novel pyran based dyes for application in dye sensitized solar cells. Dyes Pigm 2016;133:395–405; c) Bonomo M, Carella A, Centore R, Di Carlo A, Dini D. First examples of pyran based colorants as sensitizing agents of *p*-type dye-sensitized solar cells. J Electrochem Soc 2017;164: F1412–8.

[28] Chen R, Yang X, Tian H, Wang X, Hagfeldt A, Sun L. Effect of tetrahydroquinoline dyes structure on the performance of organic dye-sensitized solar cells. Chem Mater 2007;19:4007–15.

[29] Heeney M, Wagner Rt, Mcculloch I, Tierney S. Patent WO 2005111045A1, november 2005; Chem Abstr 2005;143:478363.

[30] Abaev VT, Karsanov IV, Urtaeva ZhKh, Blinokhvatov AF, Bumber AA, Okhlobystin OY. Production and properties of (4H-pyran-4-yl)diphenylphosphine oxides. Zh Obshch Khim 1990;60:1012–9.

[31] Jestin I, Frère P, Mercier N, Levillain E, Stievenard D, Roncali J. Synthesis and characterization of the electronic and electrochemical properties of thienylenevinylene oligomers with multinanometer dimensions. J Am Chem Soc 1998;120: 8150–8.

[32] a) Elandaloussi EH, Frère P, Richomme P, Orduna J, Garín J, Roncali J. Effect of chain extension on the electrochemical and electronic properties of π-conjugated soluble thienylenevinylene oligomers. J Am Chem Soc 1997;119:10774–84; b) Haynes RK, Vonwiller SC, Luderer MR. Encyclopedia of Reagents for Organic Synthesis. New York: Wiley; 2006.

[33] Horiuchi T, Miura H, Uchida S. Highly-efficient metal-free organic dyes for dye-sensitized solar cells. Chem Commun 2003:3036–7.

[34] Wang P, Klein C, Humphry-Baker R, Zakeeruddin SM, Grätzel M. A high molar extinction coefficient sensitizer for stable dye-sensitized solar cells. J Am Chem Soc 2005;127:808–9.

[35] a) Wang Z-S, Cui Y, Dan-oh Y, Kasada C, Shinpo A, Hara K. Thiophene-functionalized coumarin dye for efficient dye-sensitized solar cells: electron lifetime improved by coadsorption of deoxycholic Acid. J Phys Chem C 2007;111:7224–30; b) Zhou G, Pschirer N, Schöneboom JC, Eickemeyer F, Baumgarten M, Müllen K. Ladder-type pentaphenylene dyes for dye-sensitized solar cells. Chem Mater 2008; 20:1808–15; c) Lin L-Y, Tsai C-H, Wong K-T, Huang T-W, Hsieh L, Liu S-H et al. Organic dyes containing coplanar diphenyl-substituted dithienosilole core for efficient dye-sensitized solar cells. J Org Chem 2010;75:4778–85.

[36] Hagfeldt A, Grätzel M. Light-induced redox reactions in nanocrystalline systems. Chem Rev 1995; 95:49–68.

[37] Ba F, Robin-Le Guen F, Cabon N, Le Poul P, Golhen S, Le Poul N et al. Ferrocenyl and pyridyl methylenepyrans as potential precursors of organometallic electron-rich extended bipyrans: synthesis, characterization and crystal structure. J Organomet Chem 2010;695:235–43.

[38] Hagberg DP, Marinado T, Karlsson KM, Nonomura K, Qin P, Boschloo G et al. Tuning the HOMO and LUMO energy levels of organic chromophores for dye sensitized solar cells. J Org Chem 2007;72:9550–6.

[39] Kern R, Sastrawan R, Ferber J, Stangl R, Luther J. Modeling and interpretation of electrical impedance spectra of dye solar cells operated under open-circuit conditions. Electrochimica Acta 2002;47:4213–25.

[40] Wang Q, Moser J-E, Grätzel M. Electrochemical Impedance Spectroscopic Analysis of Dye-Sensitized Solar Cells. J Phys Chem B 2005;109:14945–53.

Highligths:

1.- Dyes with a 4*H*-pyranylidene/thienothiophene combination are reported.

2.- The photovoltaic performance is sensitive to the structure of the dyes.

3.- The highest efficiency for a 4*H*-pyranylidene-based derivative has been found: 6.41%